Approximations for Modal Coupling from Rectangular Orifices

R. Lyons Loughborough University, Department of Civil and Building Engineering, UK
J.L. Horner Loughborough University, Department of Aeronautical and Automotive Engineering

1. INTRODUCTION

Passive ventilation is one method adopted in the pursuit of low-energy solutions for buildings. A particular drawback of this method is that it allows noise to penetrate the building envelope, both as break-in and break-out noise through an opening or orifice. Designers are then faced with the problem of understanding the effects of different sound fields on either side of the orifice, of size and shape of the orifice and of any potential device within the orifice upon the sound transmitted. This is a problem that has application in many engineering disciplines and is not simply constrained to buildings. It has been a focus of the authors' work to break down this problem using an approximate modal impedance approach[1], such that designers can investigate or trial the effects of using different aperture dimensions and shapes, with or without devices of varied design. To avoid the necessity of complex computer models using fully coupled solutions the authors main endeavour is to produce simplified approximate solutions, allowing an approximate modal impedance approach to be used. These approximate impedances contain contributions from the coupled higher-order modes in the associated fields.

The work presented here is part of the ongoing research[2] and focuses upon the development of approximate expressions for rectangular orifices. In particular it concerns the contributions of the higher-order modes to the scattered and transmitted fields, to determine if a modal approach may be taken to approximate the in-duct and scattered sound fields from a rectangular orifice. Approximate solutions shown in the form of the modal contribution to the amplitude of the scattered field have been established[4]. Comparison to values obtained using established fully coupled solutions for the scattered field[3] is good and these results are also equally applicable to the transmitted field. These simplified expressions are used to determine the maximum modal contribution to the fields, based only on knowledge of mode number and orifice dimensions. This work is now expanded to include expressions that represent the energy in the modes and illustrate how different types of mode are influenced by the parameters of the orifice.

2. DESCRIPTION OF ACOUSTIC FIELD

Consider a rectangular aperture of height $2a$, width $2b$ and depth d in a rigid wall (Figure 1). For simplicity the following analysis is undertaken in terms of velocity potentials, from which the impedance may be obtained. Following Ref. 4 the velocity potential for an incident wave of arbitrary impingement angles θ and ϕ, may be given by

$$\Phi^i(x,y,z) = e^{i(k_x x + k_y y - k_z z)} \quad (1)$$

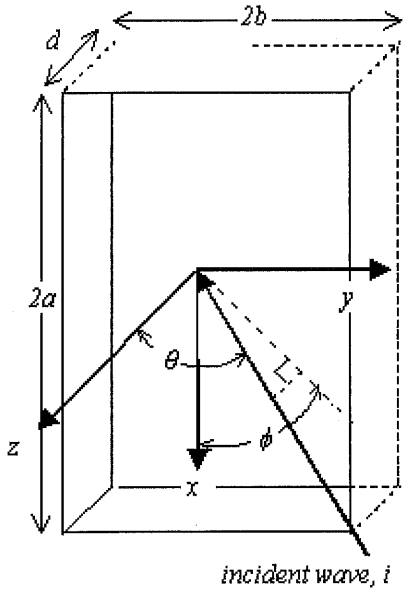

Figure 1, Co-ordinate system for Rectangular orifice in rigid plate

Where $k_x = k\cos\phi\sin\theta$, $k_y = k\sin\phi\sin\theta$ and $k_x = k\cos\theta$. A time base of $e^{-i\omega t}$ is suppressed throughout for brevity. The resulting reflected and scattered velocity potentials are given by:

$$\Phi^r(x,y,z) = e^{i(k_x x + k_y y + k_z z)} \quad (2)$$

$$\Phi^s(x,y,z) = \frac{1}{4\pi^2}\int_{-\infty}^{\infty}\int_{-\infty}^{\infty}\bar{\Phi}^s(\zeta,\eta)\, e^{-i(\zeta x + \eta y - \kappa z)}\, d\zeta\, d\eta \quad (3)$$

The scattered wave number, $\kappa = \sqrt{k^2 - \zeta^2 - \eta^2}$ and $z > 0$. Inside the duct the field is given over the depth, d, by Equation (4), for which $\xi_{mn} = \sqrt{k^2 - k_m^2 - k_n^2}$ represents the wave number in the z-direction and $k_m = \frac{m\pi}{2a}$ and $k_n = \frac{n\pi}{2b}$ are the cross-sectional wave numbers.

$$\Phi^d(x,y,z) = \sum_{m=0}^{\infty}\sum_{n=0}^{\infty}\left[c_{mn}\cos\xi_{mn}(z+d) + d_{mn}\sin\xi_{mn}(z+d)\right]\times\cos k_m(x+a)\cos k_n(y+b) \quad (4)$$

Assuming a rigid wall surrounding the aperture, the velocity potential gradients may be summed for the aperture area and regions outside. Applying a Fourier Transform, as shown by Ref. 4, to the two expressions determined from the summed velocity potential gradients yields the following expression:

$$\bar{\Phi}^s(\zeta,\eta) = -i(ab)^2\frac{\zeta\eta}{\kappa}\sum_{m=0}^{\infty}\sum_{n=0}^{\infty}\xi_{mn}\left[-c_{mn}\sin(\xi_{mn}d) - d_{mn}\cos(\xi_{mn}d)\right] F_m(\zeta a) F_n(\eta b) \quad (5)$$

This expression gives the amplitude of the scattered field, which depends on the recoil wave number in the x-direction, ζ, and the recoil wave number in the y-direction, η. As c_{mn} and d_{mn} are the amplitudes of the waves in the aperture, the term $F_m(\zeta a) F_n(\eta b)$, may be considered to drive the scattered field and is given by:

$$F_m(\zeta a)\,F_n(\eta b) = \left(\frac{(-1)^m e^{j\zeta a} - e^{-j\zeta a}}{(\zeta a)^2 - \left(m\pi/2\right)^2}\right)\left(\frac{(-1)^n e^{j\eta b} - e^{-j\eta b}}{(\eta b)^2 - \left(n\pi/2\right)^2}\right) \qquad (6)$$

As the amplitude of the scattered field depends on both m and n, each mode will give a different value of the product. It should be noted that c_{mn} and d_{mn} are determined by considering the transmitting side of the aperture and solving at all boundaries for continuity of velocity potentials and particle velocities. This will result in a set of simultaneous equations whose solution yields values for c_{mn} and d_{mn}, which include modal contributions from all modes considered in the calculation.

3. INVESTIGATION OF PRODUCT

In order to formulate an approximate expression for coupling between higher-order modes, the product, Equation (6), must be investigated as it determines the 'driving amplitude' of the scattered field. Knowledge was required of the position of the maximum response in the wave number domain, the magnitude of the maximum response and an indication of the total energy represented by the integral of the square of the product.

3.1 Position of maximum in wave number domain

It is known that the cut-on of higher-order duct modes and hence the maximum response must occur when the in-plane (cross-sectional) modal wave lengths equal the recoil wavelengths[3]. By differentiating Equation (6), it was possible to obtain an expression, Equation (7a), for the recoil wave number that gives the maximum response. Comparison of the results of Equation (7a) with the data from Equation (6) for different aperture aspect ratios and mode numbers, showed that for the case of m (or n) = 1, a maximum response always occurred at zero recoil wave number.

For m or $n > 1$: $$\zeta_{max} = \frac{m\pi}{2a}, \quad \eta_{max} = \frac{n\pi}{2b} \qquad (7a)$$

For m (or n) = 0 or 1: $$\zeta_{max} = \eta_{max} = 0 \qquad (7b)$$

For the m (or n) =1 case, the maximum value of the function does not occur at coincidence between the scattered field wave components and the duct in-plane wave components. If zero is substituted for k_m in the expression for, ζ_{mn}, the in-duct wave number in the z-direction, it may be concluded that at a fixed free wave number, the cut-on wave number of the duct, for a particular mode, is increased. This implies a change in effective length of the duct and hence an added-mass effect in the scattered field. The product, $F_m(\zeta a)\,F_n(\eta b)$, would also be present in the transmitted field[4], implying the effect would occur in both half spaces. This shift in wave number was also observed in the complementary investigation into the scattered field from a circular aperture[2]. A similar observation on the relationship between frequency and end-correction has been made by others[5].

3.2 Magnitude of the maximum value of product

The maximum value of the modulus of the product was investigated for a series of mode numbers and aperture dimensions. To uniquely describe the cross section of the aperture, the investigation considered changes in maximum response with both aperture perimeter and aperture aspect ratio. It was found that different classes of mode resulted in different controlling parameters for the magnitude of the maximum value. This behaviour of different types of modes being controlled by different parameters was also observed in the complementary investigation[2]. Note that the following expressions determine the maximum value of the magnitude of the product. The product will be real valued when *m* and *n* are both odd or are both even. If *m* is odd and *n* is even, or vice-versa, the product will be wholly imaginary.

Axial Modes

An expression has been determined[3], using curve fitting, to give the approximate maximum value of the magnitude of the product for axial modes only, with the exception of (1,0) and (0,1) modes.

$$\left|F_m(\zeta a)F_n(\eta b)\right|_{max} = \left(\frac{725\left(a/b\right)+2500}{(2a+2b)^2}\right)k_{mn}^{-1.03} \tag{8}$$

Note that $k_{mn} = \sqrt{k_m^2 + k_n^2}$. Errors of 1% or less are incurred by using the above equation. However, it was observed that the two primary axial modes, (1,0) and (0,1), were controlled by a different set of parameters. These were approximated using Equation (9) below, with absolute errors in the region of 2 - 4% over a range of typical building aperture dimensions. The closer the aspect ratio was to unity, the smaller was the value of the absolute error.

$$\left|F_m(\zeta a)F_n(\eta b)\right|_{max} = \frac{50\pi}{a^n b^m} \tag{9}$$

Tangential Modes

The maximum value for tangential modes was found to be independent of aperture dimension and wholly dependent upon mode number. The maximum value of the modulus may be approximated using the following expressions, again determined using curve fitting. The magnitude of the (1,1) was unique and taken as 0.657. Absolute errors were no greater than 2% when using Equation (10) to determine the magnitude for each mode.

$$\left|F_m(\zeta a)F_n(\eta b)\right|_{max} = c_1(mn)^{-1.03} \tag{10}$$

m (or n) = 1 : c_1 = 0.55 m (or n) > 1 : c_1 = 0.45

Thus the position of the maximum response in the wave number domain and the magnitude of the maximum response can be approximated over a range of apertures with aspect ratios from unity through to 10. From the above, it may be observed that depending upon the class of mode, either the maximum value or the position of the maximum value is fixed regardless of aperture dimension. However, consideration of the product over the whole of both recoil wave number domains, rather than at a single wave number, shows that the aperture dimensions significantly affects the product.

As the product is considered to be the driver of the scattered field then the square of the product can be considered proportional to the energy in the field. Using this it is possible to quantify the effect of aperture parameters on different classes of modes by taking the square of the product and then integrating over the wave number domains.

4. REPRESENTATION OF ENERGY IN MODES

Given the above, the energy in each mode could be represented by $\iint (F_m F_n)^2 \, d\eta \, d\zeta$. A simple approximation to this expression has been determined from the data output from a fully coupled model by considering a range of aspect ratios (*a*/*b*) from 1.0 to 10 and perimeters (2*a*+2*b*) from 3.0 to 7.0. It was observed that the energy, for all modes, was a function of mode number and as can be seen from Figure 2 was inversely proportional to both *m* and *n* modes.

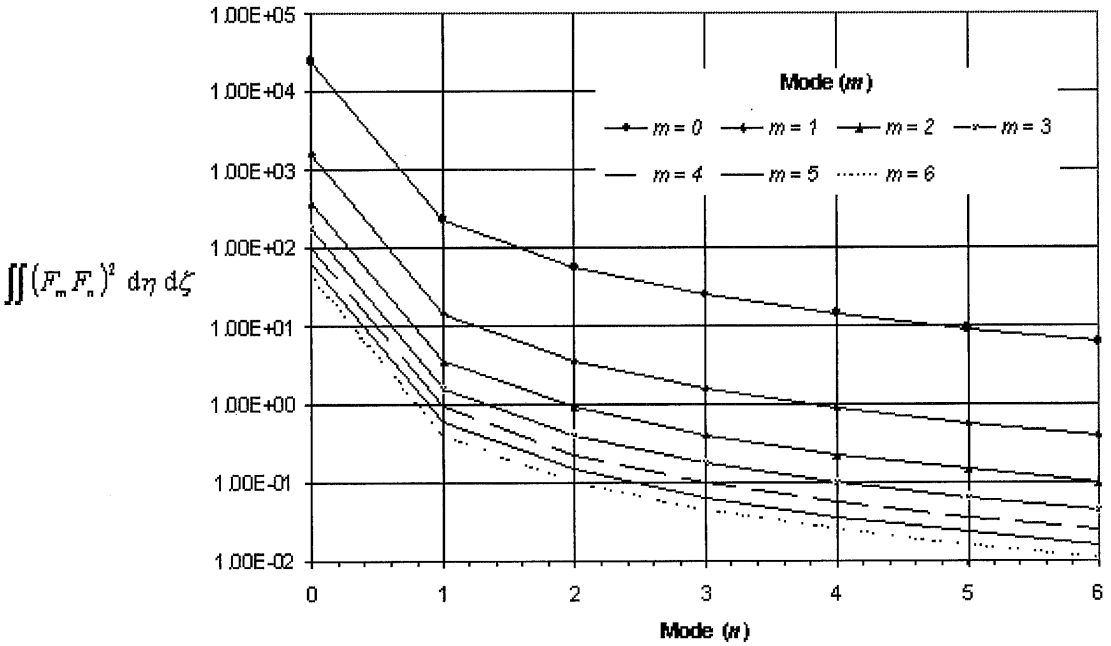

Figure 2: Value of integral of square of product for aperture of *a*/*b* = 5.8 and perimeter 3.8m.

As before the axial and tangential modes were controlled by different parameters. Using simple curve fitting routines the following approximate relationships were established for these two classes of mode.

4.1 Tangential modes

For each set of aperture parameters there was a clear relationship between mode number, *m* (or *n*) and representative energy. Again aspect ratio and perimeter were the parameters used to uniquely describe an aperture. It can be observed from Figures 3 and 4 that $\iint (F_m F_n)^2 \, d\eta \, d\zeta$ is proportional to

aspect ratio and inversely proportional to perimeter. Simple curve fitting to the whole data sets provided an expression which gives values that are representative of the energy in each mode as:

$$\iint (F_m F_n)^2 \, d\eta \, d\zeta = \frac{22.4\left(\frac{a}{b}\right)+78.4}{((2a+2b)\ mn)^2} \tag{11}$$

Relative errors in predicting the value of representative energy ranged from –3% to 4%.

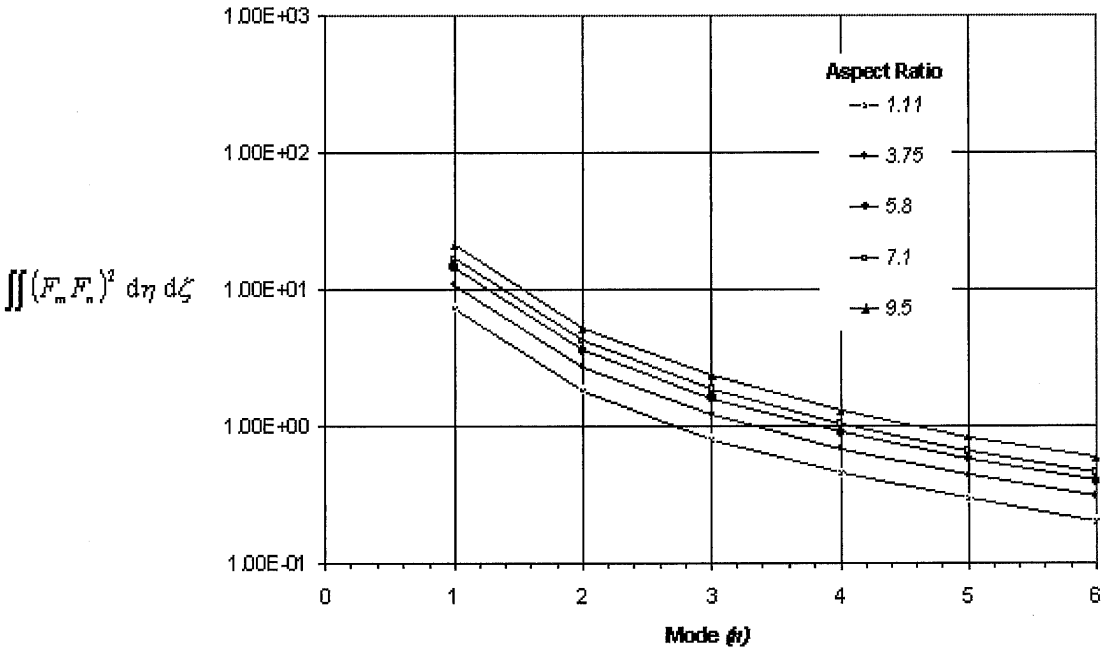

Figure 3: Value of integral of square of product for fixed perimeter of 3.8m.

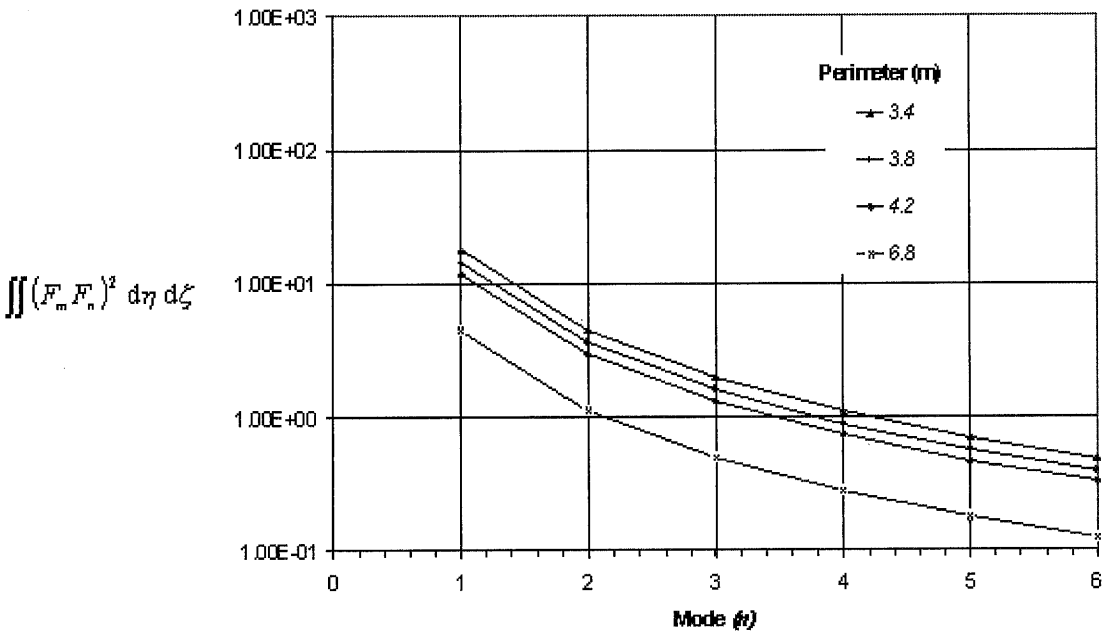

Figure 4: Value of integral of square of product for fixed aspect ratio of *a*/*b* = 5.8.

4.2 Axial modes

It is clear from Figure 2 that the axial modes do not follow the same trends as the tangential modes. The values are, however, still proportional to aspect ratio and inversely proportional to perimeter. Two expressions were determined for axial modes as shown below. Note that aspect ratio (*a*/*b*) has been defined as the major dimension over the minor dimension (i.e. $a/b \geq 1$).

For $n = 0$ modes:

$$\iint (F_m F_n)^2 \, d\eta \, d\zeta = \frac{6250\left(\frac{a}{b}\right)^{1.5}}{(2a+2b)^3 m^2} \quad (12)$$

-

For $m = 0$ modes:

$$\iint (F_m F_n)^2 \, d\eta \, d\zeta = \frac{1100\left(\frac{a}{b}+5.6\right)}{(2a+2b)^3 n^2} \quad (13)$$

Relative errors in predicting the value of representative energy ranged from –5% to +5% for Equation 12 and –1% to +2% for Equation 13. More significant errors occur using Equation 13, but only where energy levels were very small and therefore negligible.

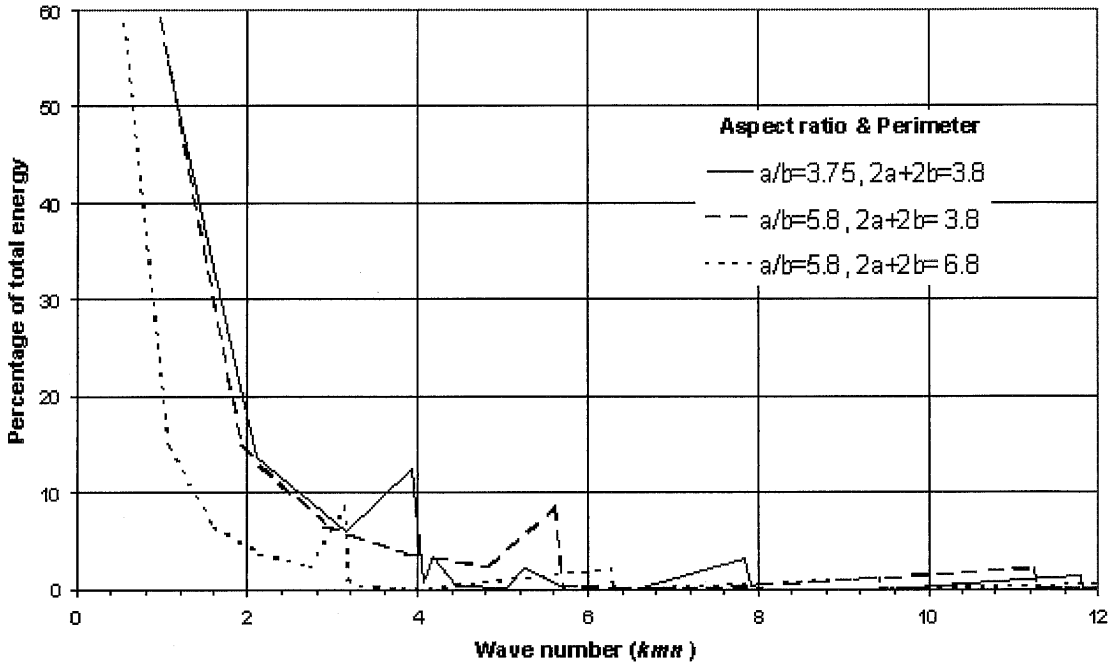

Figure 5: Percentage of total energy in first 35 modes from integrated value of square of $F_m(\zeta a)F_n(\eta b)$ indicating energy in the field.

Figure 5 shows the percentage of total energy in the first 35 modes from integrated value of square of $F_m(\zeta a)F_n(\eta b)$ indicating energy in the field versus cross-sectional wave number k_{mn} for three different aperture dimensions. Percentage energy is calculated by summing the energy in the 35 modes to get total energy and then dividing the energy of each mode by the total. The plane wave (0,0) is ignored from the calculations. The data shows that the dominant mode in each case is the (1,0) and that energy decays with increasing k_{mn}. The data does not have a smooth decay, with the axial modes being the 'peaks' in the data. This implies that for a particular modal wave number, an axial mode excited at that wave number contains more energy than a tangential mode excited at the same wave number.

It should be noted that at low wave numbers perimeter rather than aspect ratio, determines the energy contributed to the field. Thus to reduce modal energy at low wave numbers it is necessary to increase the perimeter rather than alter the aspect ratio. However, it should be noted that a change in aspect ratio leads to a shift in the energy peaks due to the axial mode contribution.

5. CONCLUSION

This paper presents a section of a larger piece of research that aims to develop an approximate modal impedance approach for performance prediction of apertures and aperture attenuating devices. This work has shown that approximate expressions can be found for rectangular apertures incurring acceptable errors, for aspect ratios from 1.0 to 10.0. These expressions provide information

upon the maximum 'driving amplitude' of the scattered field and also of the position of the maximum amplitude in the wave number domain. This magnitude depends upon the class of the mode, axial or tangential. The former magnitude is dependent upon both aspect ratio and perimeter, while the latter is independent of aperture dimension.

The main part of this work is the expressions found to represent the energy contributed to the scattered field. Again this is shown to be dependent upon the class of mode and is proportional to aspect ratio and inversely proportional to the perimeter. Importantly, it is observed that for low wave number the perimeter determines the energy contribution to the field and increasing perimeter rather than aspect ratio causes a reduction in modal energy contributed to the scattered field. Peaks in the representative energy are the result of axial modes, which will shift in wave number when the dimensions are adjusted. The expressions presented require proving over a larger data set and by application through a modal impedance model and experimental measurement.

6. REFERENCES

1. Petersson, B.A.T. Horner, J.L. and Lyons, R., "An Engineering Approach for the Acoustic Characterisation of Apertures", *Proceedings of the Institute of Acoustics*, 21(3), 1999, pp 131-138.
2. Horner, J. L, Lyons, R. and Petersson, B.A.T. 'Approximations for modal coupling in scattered fields from orifices', J.Acoust. Soc.Am 108(2) , 2000, pp 488-493.
3. Horner, J.L. and Lyons, R., 'Modal Scattering from Rectangular Orifices', *Inter-Noise 2001*, 1, 2001, pp 283-286
4. Park, H.Y. and Eom, H.J. 'Acoustic Scattering from a rectangular aperture in a thick hard screen', J Acoust. Soc. Am.101(1), 1997, pp 595-598
5. Gomperts M.C., 'The sound insulation of circular and slit shaped apertures', Acustica, 14(1), 1964, pp 1-16.